SYSTEM IDENTIFICATION AND MODELLING OF ROTARY INVERTED PENDULUM

T. Teng Fong, Z. Jamaludin and L. Abdullah
Faculty of Manufacturing Engineering, Universiti Teknikal Malaysia Melaka,
Durian Tunggal, 76100 Melaka, Malaysia

ABSTRACT

An inverted pendulum is a classic case of robust controller design. A successfully validated and precise system model would greatly enhance the performance of the controller making system identification as a major procedure in control system design. Several techniques exist in literature for system identification, and these include time domain approach and frequency domain approach. This paper gives an in-depth analysis of system identification and modelling of rotary inverted pendulum that describes the dynamic models in upright and downward position. An extensive elaboration on derivation of the mathematical model describing the physical dynamic model of the rotary inverted pendulum is described in this paper. In addition, a frequency response function (FRF) of the physical system is measured. The parametric model estimated using non-linear least square frequency domain identification approach based on the measured FRF is then applied as a mean to validate the derived mathematical model. It is concluded that based on the validation, the dynamic model and the parametric model are well fitted to the FRF measurement.

KEYWORDS: *System Identification, Rotary Inverted Pendulum, Mathematical Modelling, Linear Approximation Method, Frequency Domain Identification.*

I. INTRODUCTION

Control of under-actuated systems is difficult and has attracted much attention due to their wide-ranging applications. During the last few decades, under-actuated physical systems have drawn great interest among researchers for developing different control strategies, such as those in robotics, aerospace engineering, and marine engineering[1]. An inverted pendulum is a difficult system to control being essentially unstable. Thus, control of an inverted pendulum is one of the most important classical problems in the research interest of control engineering to improve the performance of the control system[2]. It is a well-known fact that under-actuated systems have fewer actuators than the degrees of freedom. The rotary inverted pendulum (RIP) system consists of an actuator and two degrees of freedom. The pendulum is stable when hanging downwards whereas it is naturally unstable with oscillation. Therefore, torque or force must be applied to keep it balanced to remain in inverted position. The inverted pendulum model can be applied in control of a space booster racket and a satellite, an automatic aircraft landing system, aircraft stabilization in the turbulent air flow, stabilization of a cabin in a ship and others[3].

Mathematical modelling, simulation, non-linear analysis, decision making, identification, estimation, diagnostics, and optimization have become major mainstreams in control system engineering. System identification is a general term used to describe mathematical tools and algorithms that build dynamical models from measured data[4]. Mathematical modelling is the basis of the control strategies when approaching the solution of a control problem. The physical system dynamic equations were performed analytically or numerically in solving these equations. It can be derived by the Newtonian mechanics and the Lagrange's equations of motion, the Kirchhoff's laws, and the

energy conservation principles[5]. There are many approaches when deriving the mathematical model, but Lagrange equations offer the systematic and error free way to do it[6]. The equations of motion normally were obtained by using the free body diagram referencing to Newtonian method. Linearization the non-linear model with single support point was possible performed about equilibrium point[7]. Then, the linear control theories can be applied in design and control the system. Besides that, the MATLAB GUI can be used to estimate automatically the mathematical model of the system[8]. Furthermore, parametric model, non-parametric model, black box model, white box model and linear model can be applied in system identification. The system identification was estimated using non-linear least square frequency domain identification method and H1 estimator in frequency response function (FRF)[9]. The frequency domain identification method offers several advantages compared to the time domain approach, such as data and noise reduction[10].

The aim of this paper is to extensively elaborate the identification and modelling of a rotary inverted pendulum using mathematical model validated with parametric model generated using frequency response function. The paper is organized as follows; the next section provides the system setup. Section III shows the methodology of mathematical modelling and frequency response method together with the validation result and discussion. Finally, a conclusion and future work are given in Section IV of the paper.

II. SYSTEM SETUP

TeraSoft Electro-Mechanical Engineering Control System (EMECS) is a set of electro-mechanical devices for controlling engineering research and education. The EMECS consists of three main components such as Micro-box 2000/2000C, servo-motor module, and driver circuit. The Micro-box 2000/2000C is a xPC Target machine that operates on wide variety of x86-based PC system where the system has analogue-to-digital converter (ADC), digital-to-analogue converter (DAC), general-purpose input/output (GPIO) and encoder input/output boards installed. It works as data acquisition unit with operating voltage between 9 and 36 volts. Then, the servo-motor module consists of a permanent-magnet, brushed DC motor that runs on a terminal voltage of 24 volts. Besides that, angular position of shaft of the DC motor is measured by a rotary incremental optical encoder. The encoder has a resolution of 500 counts per resolution. Figure 1 shows a schematic diagram of EMECS that includes the servo-motor module, driver circuit, Micro-box 2000/2000C and host computer. The driver circuit and the servo-motor module are connected to the Micro-Box 2000/2000C. The switching power supply is connected to the driver circuit board and AC/DC adapter is connected to the data acquisition unit. Besides, Ethernet cable is connected between host computer and the data acquisition unit[11]. The system connections of EMECS are shown in Figure 2:

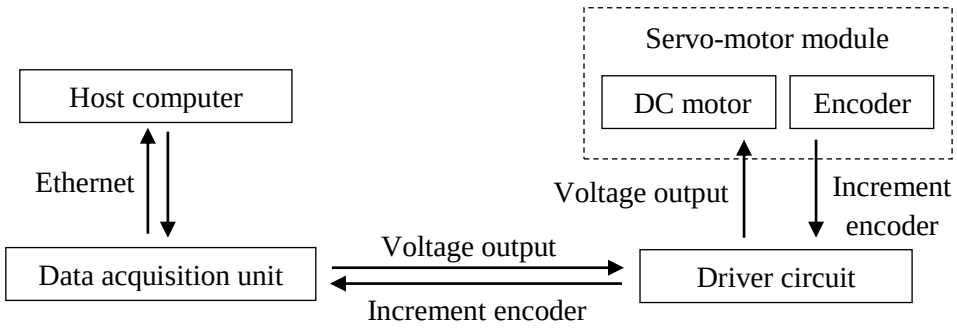

Figure 1. System setup of EMECS.

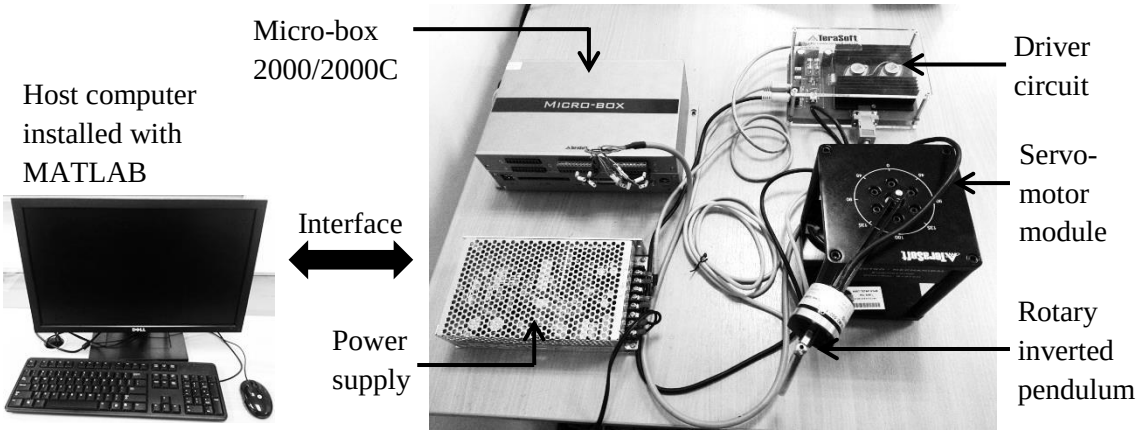

Figure 2. System connections of EMECS.

III. RESEARCH METHODOLOGY

The methodology of identification of system is described using two different methods which are mathematical modelling and non-linear least square frequency domain identification. Figure 3 shows the overall methodology of the experiment performed. This experiment involved system identification and modelling, and model validation.

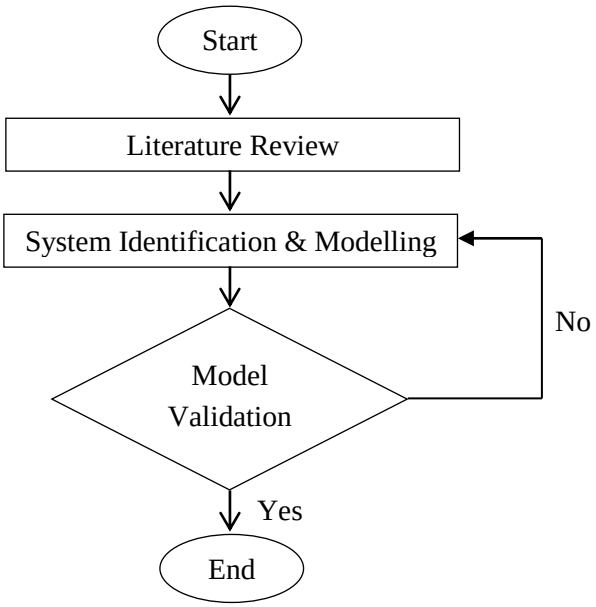

Figure 3. Flow chart of overall methodology.

These two methods were applied to compare and validate with the frequency response function (FRF) of the system. The mathematical model is obtained from formulating through equations by using measured system parameters. While non-linear least square frequency domain identification estimates parametric model that is obtained from the collected real-time data of the system FRF.

3.1. Mathematical Modelling

The RIP consists of a rigid rod called as pendulum which is rotating freely in a vertical plane with the objectives of swinging up and balancing the pendulum in the inverted position. Then, the pendulum is attached to a pivot arm that is mounted on the shaft of the servo-motor. Therefore, the pivot arm can be rotated in the horizontal plane by the servo-motor while the pendulum hangs downwards. On the other hand, the optical encoders are installed on the pivot arm and pendulum arm to detect the displacement. Figure 4 shows a free body diagram of the RIP. The system variables and parameters are defined in Table 1:

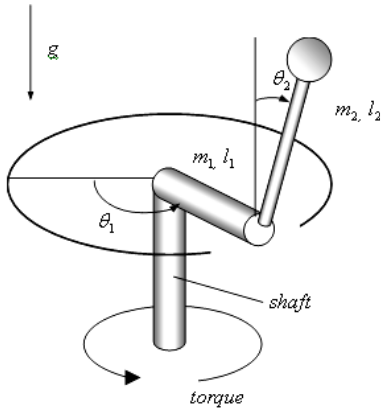

Figure 4. Simplified rotary inverted pendulum[12].

Table 1: Mechanical and electrical system parameters.

Parameter	Symbol	Numerical value
Mass of arm	m_1	$0.056\,\text{kg}$
Mass of pendulum	m_2	$0.022\,\text{kg}$
Length of arm	l_1	$0.16\,\text{m}$
Length of pendulum	l_2	$0.16\,\text{m}$
Distance to centre of arm mass	c_1	$0.08\,\text{m}$
Distance to centre of pendulum mass	c_2	$0.08\,\text{m}$
Inertia of arm	J_1	$0.00215058\,\text{kgm}^2$
Inertia of pendulum	J_2	$0.00018773\,\text{kgm}^2$
Viscous friction co-efficient of arm	C_1	$0.02\,\text{kgm}^2/\text{s}$
Viscous friction co-efficient of pendulum	C_2	$390\,\text{kgm}^2/\text{s}$
Gravitational acceleration	g	$9.8\,\text{m}/\text{s}^2$
Angular position of arm	θ_1	rad
Angular velocity of arm	$\dot{\theta}_1$	rad/s
Angular position of pendulum	θ_2	rad
Angular velocity of pendulum	$\dot{\theta}_2$	rad/s
Motor torque constant	K_t	$0.01826\,\text{Nm}/\text{A}$
Motor back-emf constant	K_b	$0.01826\,\text{Vs}/\text{rad}$
Motor driver amplifier gain	K_u	$10\,\text{V}/\text{count}$
Armature resistance	R_m	$2.5604\,\Omega$

The Lagrange's equation of motion was used to determine the non-linear system model. Then, the non-linear mathematical model was linearized to determine linearized system model which the model represented the pendulum in equilibrium point or upright position. Therefore, the linear approximation method was used in linearization of non-linear mathematical model. After that, the linearized mathematical model was converted in state-space model to determine the dynamic model of arm and pendulum as well. However, the system is unable to stabilize in upright position without a controller. Hence, the upright dynamic model required to convert in downward dynamic model for the validation purposes.

3.1.1. Non-linear Mathematical Model

In order to analyse the non-linear system, accurate mathematical model is approached to represent the system. The non-linear dynamic model describes the entire system where it gives exact relationships among all variables involved. All the linear models used for controller design are derived from the

non-linear model. A voltage signal is generated according to the designed control law and it is supplied to a PWM driver amplifier which drives the servo-motor to control the pendulum. By applying Kirchhoff's voltage law, the relation between the control torque, τ_1 and the control voltage, e is shown in Equation (1):

$$\tau_1 = \frac{K_t K_u}{R_m} e - \frac{K_t K_b}{R_m} \dot{\theta}_1 \tag{1}$$

The mathematical model of RIP system is composed of two second-order non-linear differential equations which respectively described the dynamic models of the rotary arm and the pendulum by applying Lagrange's equation of motion[13]–[15]. The equation of motion can be written in the general form in Equation (2):

$$M(\theta(t))\ddot{\theta}(t) + V_m(\theta(t), \dot{\theta}(t))\dot{\theta}(t) + G(\theta(t)) = \begin{bmatrix} \tau_1 \\ 0 \end{bmatrix} \tag{2}$$

where $\theta(t) = [\theta_1(t) \quad \theta_2(t)]^T$. In this case, the backlash of the gear of the DC motor is neglected. Equation (3) is the dynamic model of the pendulum in upright position with the motor torque characteristics described in Equation (1):

$$\begin{bmatrix} J_1 + m_2 l_1^2 + m_2 c_2^2 \sin^2\theta_2 & -m_2 l_1 c_2 \cos\theta_2 \\ -m_2 l_1 c_2 \cos\theta_2 & J_2 + m_2 c_2^2 \end{bmatrix} \begin{bmatrix} \ddot{\theta}_1 \\ \ddot{\theta}_2 \end{bmatrix} +$$

$$\begin{bmatrix} C_1 + \frac{1}{2} m_2 c_2^2 \dot{\theta}_2 \sin 2\theta_2 & m_2 l_1 c_2 \dot{\theta}_2 \sin\theta_2 + \frac{1}{2} m_2 c_2^2 \dot{\theta}_1 \sin 2\theta_2 \\ -\frac{1}{2} m_2 c_2^2 \dot{\theta}_1 \sin 2\theta_2 & C_2 \end{bmatrix} \begin{bmatrix} \dot{\theta}_1 \\ \dot{\theta}_2 \end{bmatrix} +$$

$$\begin{bmatrix} 0 \\ -m_2 c_2 g \sin\theta_2 \end{bmatrix} = \begin{bmatrix} \frac{K_t K_u}{R_m} e - \frac{K_t K_b}{R_m} \dot{\theta}_1 \\ 0 \end{bmatrix} \tag{3}$$

3.1.2. Linearization of Non-linear Mathematical Model

The linear approximation method shown in Equation (4) is based on the expansion of the non-linear function into a Taylor series [16] about the operating point and the retention of only the linear terms. For η variables, $x_1, x_2, \ldots, x_n$, it can be briefly stated as:

$$y = f(x_1, x_2, \ldots, x_n)$$

$$\bar{y} = f(\bar{x}_1, \bar{x}_2, \ldots, \bar{x}_n)$$

$$y - \bar{y} \approx (x_1 - \bar{x}_1)\frac{\partial f}{\partial x_1}\Big|_{\substack{x_1=\bar{x}_1 \\ x_2=\bar{x}_2 \\ \cdots \\ x_n=\bar{x}_n}} + (x_2 - \bar{x}_2)\frac{\partial f}{\partial x_2}\Big|_{\substack{x_1=\bar{x}_1 \\ x_2=\bar{x}_2 \\ \cdots \\ x_n=\bar{x}_n}} + \ldots + (x_n - \bar{x}_n)\frac{\partial f}{\partial x_n}\Big|_{\substack{x_1=\bar{x}_1 \\ x_2=\bar{x}_2 \\ \cdots \\ x_n=\bar{x}_n}} \tag{4}$$

The model can be linearized by considering the equilibrium state [3], [17]. When the inverted pendulum is near its equilibrium point, $\dot{\theta}_1, \theta_2, \dot{\theta}_2$ are approximately equivalent to 0 (≈ 0). Thus, using linear approximations method to linear the model as follows:

$$\dot{\theta}_1 = 0;\ \theta_2 = 0;\ \dot{\theta}_2 = 0$$

$$x_1 = \theta_2;\ x_2 = \dot{\bar{\theta}}_1;\ x_3 = \dot{\bar{\theta}}_2$$

Transform Equation (3) to Equation (5) and Equation (6):

$$\left(J_1 + m_2 l_1^2\right)\ddot{\theta}_1 + m_2 c_2^2 \ddot{\theta}_1 \sin^2\theta_2 - m_2 l_1 c_2 \ddot{\theta}_2 \cos\theta_2 + \left(C_1 + \frac{K_t K_b}{R_m}\right)\dot{\theta}_1 + m_2 c_2^2 \dot{\theta}_1 \dot{\theta}_2 \sin 2\theta_2 +$$

$$m_2 l_1 c_2 \dot{\theta}_2^2 \sin\theta_2 - \frac{K_t K_u}{R_m} e = 0 \tag{5}$$

$$-m_2 l_1 c_2 \ddot{\theta}_1 \cos\theta_2 + \left(J_2 + m_2 c_2^2\right)\ddot{\theta}_2 - \tfrac{1}{2} m_2 c_2^2 \dot{\theta}_1^2 \sin 2\theta_2 + C_2 \dot{\theta}_2 - m_2 c_2 g \sin\theta_2 = 0 \tag{6}$$

For Equation (5), let

$$y = f(\theta_2, \dot{\theta}_1, \dot{\theta}_2)$$

$$y = \left(J_1 + m_2 l_1^2\right)\ddot{\theta}_1 + m_2 c_2^2 \ddot{\theta}_1 \sin^2\theta_2 - m_2 l_1 c_2 \ddot{\theta}_2 \cos\theta_2 + \left(C_1 + \frac{K_t K_b}{R_m}\right)\dot{\theta}_1 + m_2 c_2^2 \dot{\theta}_1 \dot{\theta}_2 \sin 2\theta_2 +$$

$$m_2 l_1 c_2 \dot{\theta}_2^2 \sin\theta_2 - \frac{K_t K_u}{R_m} e \quad (7)$$

$$\bar{y} = f\left(\bar{\theta}_2, \bar{\dot{\theta}}_1, \bar{\dot{\theta}}_2\right) = f(0,0,0)$$

$$\bar{y} = \left(J_1 + m_2 l_1^2\right)\ddot{\theta}_1 - m_2 l_1 c_2 \ddot{\theta}_2 - \frac{K_t K_u}{R_m} e \quad (8)$$

$$\frac{\partial y}{\partial \theta_2} = 2m_2 c_2^2 \ddot{\theta}_1 \sin\theta_2 \cos\theta_2 + m_2 l_1 c_2 \ddot{\theta}_2 \sin\theta_2 + 2m_2 c_2^2 \dot{\theta}_1 \dot{\theta}_2 \cos 2\theta_2 + m_2 l_1 c_2 \dot{\theta}_2^2 \cos\theta_2$$

$$\left.\frac{\partial y}{\partial \theta_2}\right|_{\substack{\theta_2=0 \\ \dot{\theta}_1=0 \\ \dot{\theta}_2=0}} = 0 \quad (9)$$

$$\frac{\partial y}{\partial \dot{\theta}_1} = C_1 + \frac{K_t K_b}{R_m} + m_2 c_2^2 \dot{\theta}_2 \sin 2\theta_2$$

$$\left.\frac{\partial y}{\partial \dot{\theta}_1}\right|_{\substack{\theta_2=0 \\ \dot{\theta}_1=0 \\ \dot{\theta}_2=0}} = C_1 + \frac{K_t K_b}{R_m} \quad (10)$$

$$\frac{\partial y}{\partial \dot{\theta}_2} = m_2 c_2^2 \dot{\theta}_1 \sin 2\theta_2 + 2m_2 l_1 c_2 \dot{\theta}_2 \sin\theta_2$$

$$\left.\frac{\partial y}{\partial \dot{\theta}_2}\right|_{\substack{\theta_2=0 \\ \dot{\theta}_1=0 \\ \dot{\theta}_2=0}} = 0 \quad (11)$$

$$y = \bar{y} + (\theta_2 - 0)\left.\frac{\partial y}{\partial \theta_2}\right|_{\substack{\theta_2=0 \\ \dot{\theta}_1=0 \\ \dot{\theta}_2=0}} + (\dot{\theta}_1 - 0)\left.\frac{\partial y}{\partial \dot{\theta}_1}\right|_{\substack{\theta_2=0 \\ \dot{\theta}_1=0 \\ \dot{\theta}_2=0}} + (\dot{\theta}_2 - 0)\left.\frac{\partial y}{\partial \dot{\theta}_2}\right|_{\substack{\theta_2=0 \\ \dot{\theta}_1=0 \\ \dot{\theta}_2=0}}$$

$$y = \left(J_1 + m_2 l_1^2\right)\ddot{\theta}_1 - m_2 l_1 c_2 \ddot{\theta}_2 - \frac{K_t K_u}{R_m} e + \left(C_1 + \frac{K_t K_b}{R_m}\right)\dot{\theta}_1 \quad (12)$$

Therefore, Equation (13) is linearized Equation (5) yields:

$$\left(J_1 + m_2 l_1^2\right)\ddot{\theta}_1 - m_2 l_1 c_2 \ddot{\theta}_2 + \left(C_1 + \frac{K_t K_b}{R_m}\right)\dot{\theta}_1 - \frac{K_t K_u}{R_m} e = 0 \quad (13)$$

For Equation (6), repeating the steps from Equation (7) to Equation (12). Therefore, Equation (14) is linearized Equation (6) yields:

$$-m_2 l_1 c_2 \ddot{\theta}_1 + \left(J_2 + m_2 c_2^2\right)\ddot{\theta}_2 + C_2 \dot{\theta}_2 - m_2 c_2 g \theta_2 = 0 \quad (14)$$

In matrix form Equation (15), Equation (13) and Equation (14) can be written as:

$$\begin{bmatrix} J_1 + m_2 l_1^2 & -m_2 l_1 c_2 \\ -m_2 l_1 c_2 & J_2 + m_2 c_2^2 \end{bmatrix}\begin{bmatrix} \ddot{\theta}_1 \\ \ddot{\theta}_2 \end{bmatrix} + \begin{bmatrix} C_1 + \frac{K_t K_b}{R_m} & 0 \\ 0 & C_2 \end{bmatrix}\begin{bmatrix} \dot{\theta}_1 \\ \dot{\theta}_2 \end{bmatrix} + \begin{bmatrix} 0 & 0 \\ 0 & -m_2 c_2 g \end{bmatrix}\begin{bmatrix} \theta_1 \\ \theta_2 \end{bmatrix} = \begin{bmatrix} \frac{K_t K_u}{R_m} \\ 0 \end{bmatrix} e \quad (15)$$

3.1.3. Continuous-time State-space Model

The state-space model [18] will be represented the dynamic model with the pendulum in the upright position. This model can be determined from the linearized model in Equation (15). A system is represented in state-space by the following equations:

$$\dot{x} = Ax + Bu$$
$$y = Cx + Du \quad (16)$$

Define the state variables as follows:

$$\begin{bmatrix} x_1 & x_2 & x_3 & x_4 \end{bmatrix}^T = \begin{bmatrix} \theta_1 & \theta_2 & \dot{\theta}_1 & \dot{\theta}_2 \end{bmatrix}^T$$

$$\left(J_1 + m_2 l_1^2\right)\dot{x}_3 - m_2 l_1 c_2 \dot{x}_4 + \left(C_1 + \frac{K_t K_b}{R_m}\right)x_3 = \frac{K_t K_u}{R_m} u \tag{17}$$

$$-m_2 l_1 c_2 \dot{x}_3 + \left(J_2 + m_2 c_2^2\right)\dot{x}_4 + C_2 x_4 - m_2 c_2 g x_2 = 0 \tag{18}$$

Solve the two variables equations using substitution method to eliminate one of the variables by replacement when solving a system of equations. For Equation (18), let

$$\dot{x}_4 = \frac{m_2 l_1 c_2 \dot{x}_3 - C_2 x_4 + m_2 c_2 g x_2}{J_2 + m_2 c_2^2} \tag{19}$$

Substitute Equation (19) in Equation (17), $\dot{x}_3$ yields Equation (20):

$$\dot{x}_3 = \frac{-m_2 l_1 c_2 C_2 x_4 - \left(J_2 + m_2 c_2^2\right)\left(C_1 + \frac{K_t K_b}{R_m}\right)x_3 + m_2^2 l_1 c_2^2 g x_2 + \left(J_2 + m_2 c_2^2\right)\frac{K_t K_u}{R_m} u}{\left(J_1 + m_2 l_1^2\right)\left(J_2 + m_2 c_2^2\right) - m_2^2 l_1^2 c_2^2} \tag{20}$$

For Equation (18), let

$$\dot{x}_3 = \frac{\left(J_2 + m_2 c_2^2\right)\dot{x}_4 + C_2 x_4 - m_2 c_2 g x_2}{m_2 l_1 c_2} \tag{21}$$

Substitute Equation (21) in Equation (17), $\dot{x}_4$ yields Equation (22):

$$\dot{x}_4 = \frac{-\left(J_1 + m_2 l_1^2\right)C_2 x_4 - \left(m_2 l_1 c_2\right)\left(C_1 + \frac{K_t K_b}{R_m}\right)x_3 + \left(J_1 + m_2 l_1^2\right)\left(m_2 c_2 g\right)x_2 + \left(m_2 l_1 c_2\right)\frac{K_t K_u}{R_m} u}{\left(J_1 + m_2 l_1^2\right)\left(J_2 + m_2 c_2^2\right) - m_2^2 l_1^2 c_2^2} \tag{22}$$

With the physical parameters of the system mentioned above, the state-space model is represented the linearized system in upright position as stated in equation (24):

$$\dot{x}_1 = x_3$$

$$\dot{x}_2 = x_4$$

$$\dot{x}_3 = \frac{-m_2 l_1 c_2 C_2 x_4 - \left(J_2 + m_2 c_2^2\right)\left(C_1 + \frac{K_t K_b}{R_m}\right)x_3 + m_2^2 l_1 c_2^2 g x_2 + \left(J_2 + m_2 c_2^2\right)\frac{K_t K_u}{R_m} u}{\left(J_1 + m_2 l_1^2\right)\left(J_2 + m_2 c_2^2\right) - m_2^2 l_1^2 c_2^2}$$

$$\dot{x}_4 = \frac{-\left(J_1 + m_2 l_1^2\right)C_2 x_4 - \left(m_2 l_1 c_2\right)\left(C_1 + \frac{K_t K_b}{R_m}\right)x_3 + \left(J_1 + m_2 l_1^2\right)\left(m_2 c_2 g\right)x_2 + \left(m_2 l_1 c_2\right)\frac{K_t K_u}{R_m} u}{\left(J_1 + m_2 l_1^2\right)\left(J_2 + m_2 c_2^2\right) - m_2^2 l_1^2 c_2^2} \tag{23}$$

$$\begin{bmatrix} \dot{x}_1 \\ \dot{x}_2 \\ \dot{x}_3 \\ \dot{x}_4 \end{bmatrix} = \begin{bmatrix} 0 & 0 & 1 & 0 \\ 0 & 0 & 0 & 1 \\ 0 & 5.9796 & -8.1419 & -0.1098 \\ 0 & 57.6254 & -6.9788 & -1.0584 \end{bmatrix}\begin{bmatrix} x_1 \\ x_2 \\ x_3 \\ x_4 \end{bmatrix} + \begin{bmatrix} 0 \\ 0 \\ 28.8442 \\ 24.7236 \end{bmatrix} u$$

$$y = \begin{bmatrix} 0 & 1 & 0 & 0 \end{bmatrix}\begin{bmatrix} x_1 \\ x_2 \\ x_3 \\ x_4 \end{bmatrix} \tag{24}$$

In addition, the dynamic model for downward position of pendulum is formulated in the following formulas. Defined α_2 to be the angular position of the pendulum that taken from the downward vertical. Thus, the relationship between terms involving θ_2 and α_2 can be well defined as follows:

$\theta_2 = \alpha_2 - \pi$; $\dot{\theta}_2 = \dot{\alpha}_2$; $\ddot{\theta}_2 = \ddot{\alpha}_2$;

$cos\theta_2 = cos(\alpha_2 - \pi) = -cos\alpha_2$;
$sin\,\theta_2 = sin(\alpha_2 - \pi) = -sin\,\alpha_2$;
$\sin 2\theta_2 = \sin 2(\alpha_2 - \pi) = \sin(2\alpha_2 - 2\pi) = \sin 2\alpha_2$
By substitute the terms above in Equation (3) yields:

$$\begin{bmatrix} J_1 + m_2 l_1^2 + m_2 c_2^2 (-sin\,\alpha_2)^2 & -m_2 l_1 c_2 (-cos\,\alpha_2) \\ -m_2 l_1 c_2 (-cos\,\alpha_2) & J_2 + m_2 c_2^2 \end{bmatrix} \begin{bmatrix} \ddot{\theta}_1 \\ \ddot{\alpha}_2 \end{bmatrix} +$$

$$\begin{bmatrix} C_1 + \frac{1}{2} m_2 c_2^2 \dot{\alpha}_2\, sin\,2\alpha_2 & m_2 l_1 c_2 \dot{\alpha}_2 (-sin\,\alpha_2) + \frac{1}{2} m_2 c_2^2 \dot{\theta}_1\, sin\,2\alpha_2 \\ -\frac{1}{2} m_2 c_2^2 \dot{\theta}_1\, sin\,2\alpha_2 & C_2 \end{bmatrix} \begin{bmatrix} \dot{\theta}_1 \\ \dot{\alpha}_2 \end{bmatrix} +$$

$$\begin{bmatrix} 0 \\ -m_2 c_2 g (-sin\,\alpha_2) \end{bmatrix} = \begin{bmatrix} \frac{K_t K_u}{R_m} e - \frac{K_t K_b}{R_m} \dot{\theta}_1 \\ 0 \end{bmatrix} \quad (25)$$

Therefore, the dynamic model for downward position of the pendulum with the motor torque characteristics is compactly formulated in Equation (26):

$$\begin{bmatrix} J_1 + m_2 l_1^2 + m_2 c_2^2\, sin^2\,\alpha_2 & m_2 l_1 c_2\, cos\,\alpha_2 \\ m_2 l_1 c_2\, cos\,\alpha_2 & J_2 + m_2 c_2^2 \end{bmatrix} \begin{bmatrix} \ddot{\theta}_1 \\ \ddot{\alpha}_2 \end{bmatrix} +$$

$$\begin{bmatrix} C_1 + \frac{1}{2} m_2 c_2^2 \dot{\alpha}_2\, sin\,2\alpha_2 & -m_2 l_1 c_2 \dot{\alpha}_2\, sin\,\alpha_2 + \frac{1}{2} m_2 c_2^2 \dot{\theta}_1\, sin\,2\alpha_2 \\ -\frac{1}{2} m_2 c_2^2 \dot{\theta}_1\, sin\,2\alpha_2 & C_2 \end{bmatrix} \begin{bmatrix} \dot{\theta}_1 \\ \dot{\alpha}_2 \end{bmatrix} +$$

$$\begin{bmatrix} 0 \\ m_2 c_2 g\, sin\,\alpha_2 \end{bmatrix} = \begin{bmatrix} \frac{K_t K_u}{R_m} e - \frac{K_t K_b}{R_m} \dot{\theta}_1 \\ 0 \end{bmatrix} \quad (26)$$

In order to obtain state-space model for downward position, repeating the steps of formulation for the state-space model in upright position from Equation (4) to Equation (24). As a result, the linearized system model of downward position in state-space model as shown in Equation (27). It is followed by the model with the physical parameters as presented in Equation (28):

$\dot{x}_1 = x_3$
$\dot{x}_2 = x_4$

$$\dot{x}_3 = \frac{m_2 l_1 c_2 C_2 x_4 - \left(J_2 + m_2 c_2^2\right)\left(C_1 + \frac{K_t K_b}{R_m}\right) x_3 + m_2^2 l_1 c_2^2 g x_2 + \left(J_2 + m_2 c_2^2\right)\frac{K_t K_u}{R_m} u}{\left(J_1 + m_2 l_1^2\right)\left(J_2 + m_2 c_2^2\right) - m_2^2 l_1^2 c_2^2}$$

$$\dot{x}_4 = \frac{-\left(J_1 + m_2 l_1^2\right) C_2 x_4 + \left(m_2 l_1 c_2\right)\left(C_1 + \frac{K_t K_b}{R_m}\right) x_3 - \left(J_1 + m_2 l_1^2\right)\left(m_2 c_2 g\right) x_2 - \left(m_2 l_1 c_2\right)\frac{K_t K_u}{R_m} u}{\left(J_1 + m_2 l_1^2\right)\left(J_2 + m_2 c_2^2\right) - m_2^2 l_1^2 c_2^2} \quad (27)$$

$$\begin{bmatrix} \dot{x}_1 \\ \dot{x}_2 \\ \dot{x}_3 \\ \dot{x}_4 \end{bmatrix} = \begin{bmatrix} 0 & 0 & 1 & 0 \\ 0 & 0 & 0 & 1 \\ 0 & 5.9796 & -8.1419 & 0.1098 \\ 0 & -57.6254 & 6.9788 & -1.0584 \end{bmatrix} \begin{bmatrix} x_1 \\ x_2 \\ x_3 \\ x_4 \end{bmatrix} + \begin{bmatrix} 0 \\ 0 \\ 28.8442 \\ -24.7236 \end{bmatrix} u$$

$$y = \begin{bmatrix} 0 & 1 & 0 & 0 \end{bmatrix} \begin{bmatrix} x_1 \\ x_2 \\ x_3 \\ x_4 \end{bmatrix} \quad (28)$$

3.2. Frequency Response Method

The system is identified based on actual data captured using several series of experiments. This approach is used to figure out the parametric model based on frequency response function (FRF) measurement [9]. System is excited using band-limited white noise signal [10] while the input voltage to the motor and the angular positions of the pendulum were measured and recorded in Micro-box as shown in Figure 5.

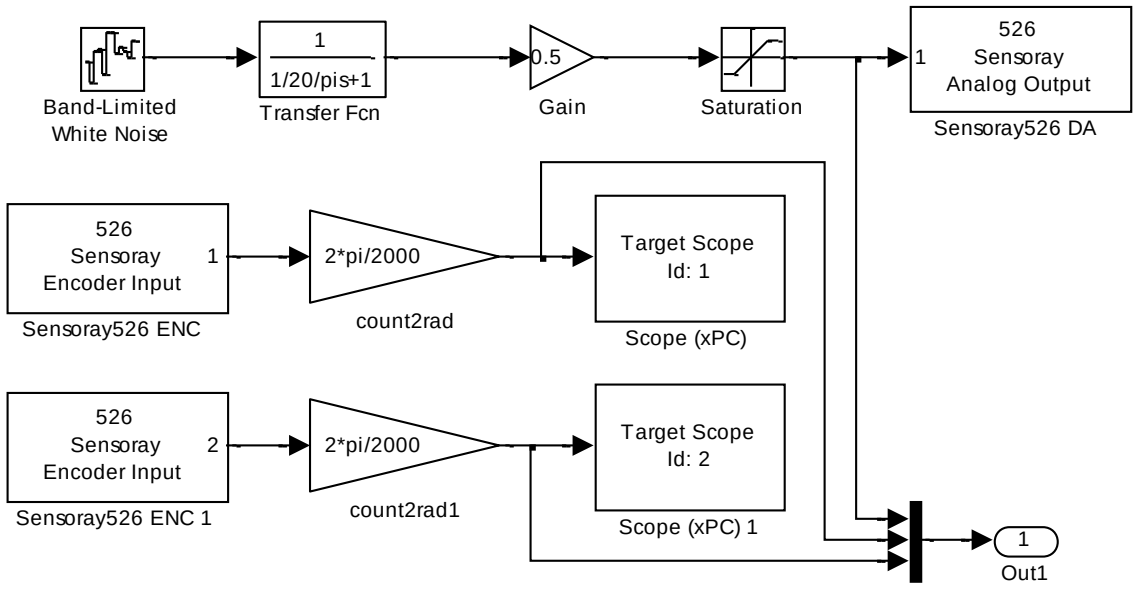

Figure 5. Input signal and schematic diagram of system identification.

The input of the motor voltage and the output of the angular position of the pendulum are served as the input for the frequency response function (FRF). By determining the input values, FRF of the system can be estimated. The measurement was collected with 1000Hz of sampling frequency and 180 seconds of total duration. The frequency response function of the system was then estimated using H1 estimator with a Hanning window applied. A system transfer function with a second order numerator value and a fourth order denominator is identified (29). This transfer function relates the input voltage to output angular position of the pendulum:

$$G(s)=\frac{0.0277s^3-24.92s^2-323.4s+164.6}{s^4+15.28s^3+200.6s^2+1589s+6548} \quad (29)$$

Figure 6 shows the validation result between two methods and the FRF. The downward dynamic model (28) and the parametric model (29) are plotted to compare and validate with the FRF of the system.

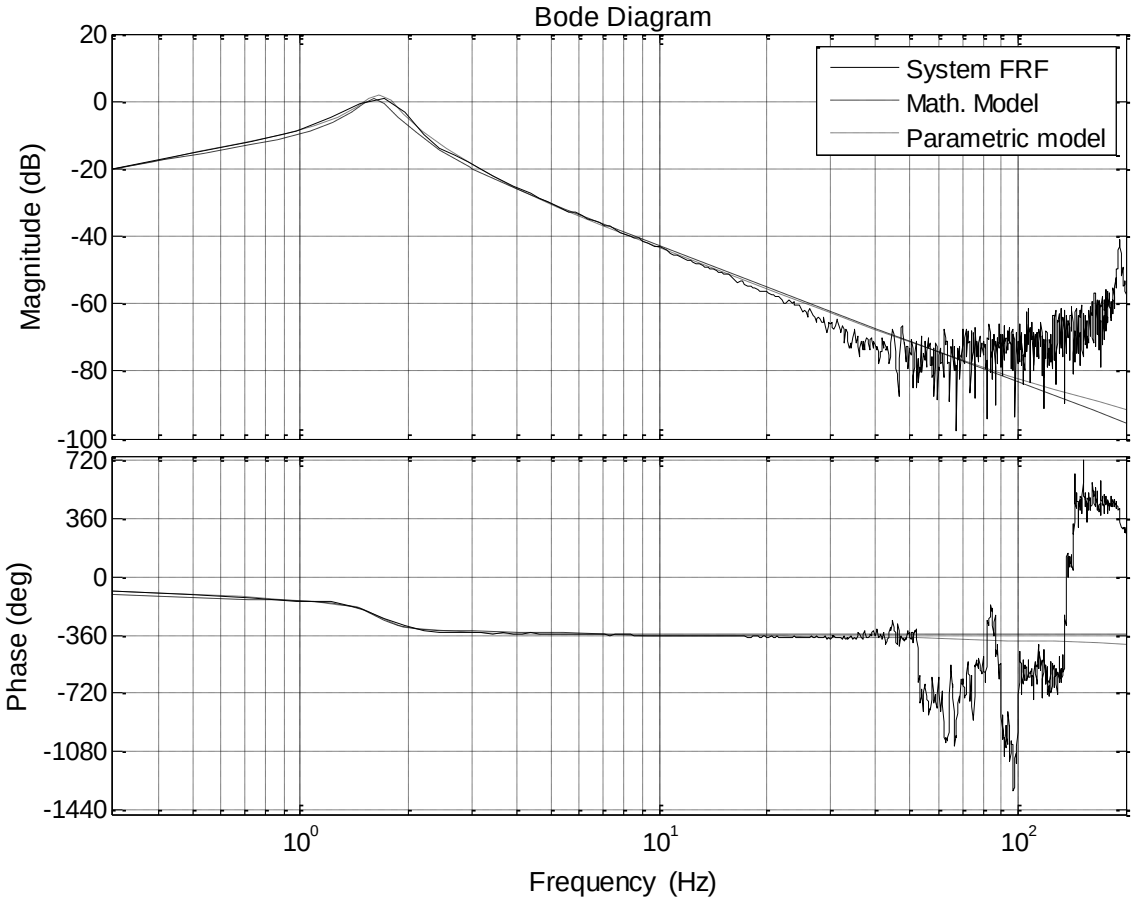

Figure 6. Validation of a system model.

According to the result obtained, both two methods are fitted to the FRF of the system. Both models are fitted up to 23Hz of frequency with the acceptable validation. This is because the EMECS runs in low band of frequency and not exceeding 23Hz in actual experiment. Besides, the models can be fitted to higher frequency, but the order of transfer function of the models will be increased. This will further add to the complexity of the model, so it is better to maintain the order of the model as low as possible at the same time fulfilling the design requirement. Both models have second order numerator and fourth order denominator. Therefore, the formulation of downward dynamic model through mathematical modelling is validated which the model can be represented the system for simulation purposes in controller design. The parametric model that obtained using the frequency response method could as well be applied to represent the system model.

IV. CONCLUSION AND FUTURE WORK

It is concluded that the derived mathematical model describes extensively and closely the physical dynamic of the rotary inverted pendulum system. The accuracy and validity of this model however could be further enhanced by including other previously neglected parameters such as vibration, friction, wind and other disturbance signals that are hard to measure. The frequency response method offers greater advantage since it captures all the dynamic behaviour of the system as function of different frequencies. Both models could be applied in design of controller for this inverted pendulum system. The author is currently developing and analysing optimum linear quadratic regulator (LQR) controller for balance control. The performance of the controller designed at this stage could further validate the accuracy of the model derived in this work.

V. ACKNOWLEDGEMENTS

The authors would like to thank the Faculty of Manufacturing Engineering, Universiti Teknikal Malaysia Melaka (UTeM) that provided the laboratory facilities and equipment supports. Also, this research is supported by the scholarship from the Centre for Graduate Studies of the Universiti Teknikal Malaysia Melaka (UTeM).

REFERENCES

[1] N. S. Ozbek & M. O. Efe, (2010) "Swing up and stabilization control experiments for a rotary inverted pendulum— An educational comparison", in *2010 IEEE International Conference on Systems, Man and Cybernetics*, pp. 2226–2231.
[2] L. B. Prasad, B. Tyagi & H. O. Gupta, (2011) "Optimal control of nonlinear inverted pendulum dynamical system with disturbance input using PID controller & LQR", in *2011 IEEE International Conference on Control System, Computing and Engineering*, pp. 540–545.
[3] K. Barya & S. Tiwari, (2010) "Comparison of LQR and Robust Controllers for stabilizing Inverted Pendulum System", in *2010 IEEE International Conference on Communication Control and Computing Technologies (ICCCCT)*, pp. 300–304.
[4] J. Pintelon, R. & Schoukens (2012) *System identification: A frequency domain approach – 2nd edition*. John Wiley & Sons, Inc.
[5] M. Akhtaruzzaman & A. A. Shafie, (2010) "Modeling and control of a rotary inverted pendulum using various methods, comparative assessment and result analysis", in *2010 IEEE International Conference on Mechatronics and Automation*, pp. 1342–1347.
[6] P. Ernest & P. Horacek, (2011) "Algorithms for control of a rotating pendulum," in *Proc. of the 19th IEEE Mediterranean Conf. on Control and Aut (MED'11), Corfu, Greece. 2011,* no. 102.
[7] P. Xue & W. Wei, (2010) "An Analysis on the Kinetic Model of a Rotary Inverted Pendulum, and Its Intelligent Control", in *2010 International Conference on Computational and Information Sciences*, pp. 978–981.
[8] S. Jadlovska & J. Sarnovsky, (2012) "A complex overview of the rotary single inverted pendulum system," in *2012 ELEKTRO*, pp. 305–310.
[9] T. H. Chiew, Z. Jamaludin, A. Y. B. Hashim, N. A. Rafan & L. Abdullah, (2013) "Identification of Friction Models for Precise Positioning System in Machine Tools", in *Procedia Engineering*, vol. 53, pp. 569–578.
[10] L. Abdullah, Z. Jamaludin, T. H. Chiew, N. A. Rafan & M. S. S. Mohamed, (2012) "System Identification of XY Table Ballscrew Drive Using Parametric and Non Parametric Frequency Domain Estimation Via Deterministic Approach", in *Procedia Engineering*, vol. 41, no. Iris, pp. 567–574.
[11] Solution4U (2009) *Electro-Mechanical Engineering Control System user's manual*, TeraSoft, Inc.
[12] A. A. Shojaei, M. F. Othman, R. Rahmani & M. R. Rani, (2011) "A Hybrid Control Scheme for a Rotational Inverted Pendulum", in *2011 UKSim 5th European Symposium on Computer Modeling and Simulation*, pp. 83–87.
[13] S. Anvar, (2010) "Design and implementation of sliding mode-state feedback control for stabilization of Rotary Inverted Pendulum", in *2010 International Conference on Control Automation and Systems (ICCAS)*, pp. 1952–1957.
[14] J. A. Acosta, (2010) "Furuta's Pendulum: A Conservative Nonlinear Model for Theory and Practise", *Math. Probl. Eng.*, vol. 2010, pp. 1–29.
[15] J.-H. Li, (2013) "Composite fuzzy control of a rotary inverted pendulum", in *2013 IEEE International Symposium on Industrial Electronics*, pp. 1–5.
[16] S. Jadlovska & J. Sarnovsky, (2013) "Application of the state-dependent Riccati equation method in nonlinear control design for inverted pendulum systems", in *2013 IEEE 11th International Symposium on Intelligent Systems and Informatics (SISY)*, vol. 0, no. 1, pp. 209–214.
[17] P. Kumar, O. N. Mehrotra & J. Mahto, (2013) "Classical , Smart And Modern Controller Design Of Inverted Pendulum", *Int. J. Eng. Res. Appl.*, vol. 3, no. 2, pp. 1663–1672.
[18] A. Rybovic, M. Priecinsky, M. Paskala & A. Mechanical, (2012) "Control of the Inverted Pendulum Using State Feedback Control," in *2012 ELEKTRO*, pp. 145–148.

AUTHORS

Tang Teng Fong received the B.Eng. degree in manufacturing engineering from Universiti Teknikal Malaysia Melaka, Durian Tunggal, Malaysia, in 2012. He is currently pursuing M.Sc. degree in manufacturing engineering from Universiti Teknikal Malaysia Melaka, Durian Tunggal, Malaysia. His field of study is in control systems.

Zamberi Jamaludin, received the B.Eng. degree in chemical engineering from Lakehead University, Thunder Bay, Ontario, Canada, in 1997, the M.Eng. degree in manufacturing systems from National University of Malaysia, Bangi, Malaysia, in 2001, and the Ph.D. degree in engineering from Katholieke Universiteit Leuven, Leuven, Belgium, in 2008. He is currently a Senior Lecturer with the Department of Robotic and Automation, Faculty of Manufacturing Engineering, Universiti Teknikal Malaysia Melaka, Durian Tunggal, Malaysia. His fields of interest are in control systems, motion control, mechatronics, and robotics.

Lokman Abdullah received the B.Eng. degree in manufacturing engineering from International Islamic University Malaysia, Selayang, Malaysia, in 2005, the M.Sc. degree in manufacturing system engineering from Coventry University, Coventry, United Kingdom, in 2008. He is currently a Lecturer with the Department of Robotic and Automation, Faculty of Manufacturing Engineering, Universiti Teknikal Malaysia Melaka, Durian Tunggal, Malaysia. His fields of interest are in control systems and RFID.